Am J Physiol Lung Cell Mol Physiol 291: L559–L565, 2006.
First published April 7, 2006; doi:10.1152/ajplung.00498.2005.

TRANSLATIONAL PHYSIOLOGY

Peristalsis of airway smooth muscle is developmentally regulated and uncoupled from hypoplastic lung growth

E. C. Jesudason,[1] N. P. Smith,[1] M. G. Connell,[1] D. G. Spiller,[2] M. R. H. White,[2] D. G. Fernig,[3] and P. D. Losty[1]

[1]*Division of Child Health,* [2]*Centre for Cell Imaging, and* [3]*The Molecular Medicine Group, University of Liverpool, Liverpool, United Kingdom*

Submitted 28 November 2005; accepted in final form 6 April 2006

Jesudason, E. C., N. P. Smith, M. G. Connell, D. G. Spiller, M. R. H. White, D. G. Fernig, and P. D. Losty. Peristalsis of airway smooth muscle is developmentally regulated and uncoupled from hypoplastic lung growth. *Am J Physiol Lung Cell Mol Physiol* 291: L559–L565, 2006. First published April 7, 2006; doi:10.1152/ajplung.00498.2005.—Prenatal airway smooth muscle (ASM) peristalsis appears coupled to lung growth. Moreover, ASM progenitors produce fibroblast growth factor-10 (FGF-10) for lung morphogenesis. Congenital diaphragmatic hernia (CDH) is associated with lung hypoplasia, FGF-10 deficiency, and postnatal ASM dysfunction. We hypothesized ASM dysfunction emerges in tandem with, and may contribute toward, the primordial lung hypoplasia that precedes experimental CDH. Spatial origin and frequency of ASM peristaltic waves were measured in normal and hypoplastic rat lungs cultured from *day 13.5* of gestation (lung hypoplasia was generated by nitrofen dosing of pregnant dams). Longitudinal lung growth was assayed by bud counts and tracing photomicrographs of cultures. Coupling of lung growth and peristalsis was tested by stimulation studies using serum, FGF-10, or nicotine and inhibition studies with nifedipine or U0126 (MEK1/2 inhibitor). In normal lung, ASM peristalsis is developmentally regulated: proximal ASM becomes quiescent (while retaining capacity for cholinergic-stimulated peristalsis). However, in hypoplastic lung, spontaneous proximal ASM activity persists. FGF-10 corrects this aberrant ASM activity in tandem with improved growth. Stimulation and inhibition studies showed that, unlike normal lung, changes in growth or peristalsis are not consistently accompanied by parallel modulation of the other. ASM peristalsis undergoes FGF-10-regulated spatiotemporal development coupled to lung growth: this process is disrupted early in lung hypoplasia. ASM dysfunction emerges in tandem with and may therefore contribute toward lung hypoplasia in CDH.

lung branching morphogenesis; congenital diaphragmatic hernia

DOES AIRWAY SMOOTH MUSCLE (ASM) have a purpose? It has been suggested that no harm would result were it not to exist (32). Furthermore, ASM has been described as "the appendix of the lung," implying it causes only trouble (24). The pivotal role of ASM in reactive airways disease certainly makes this view persuasive (5).

Nevertheless, several pieces of evidence indicate that ASM plays a key role during lung development. From embryogenesis onward, ASM elaborates smooth muscle actin (SMA) and is mechanically active: spontaneous periodic calcium waves spread via ASM immediately before a propagating peristaltic wave (airway peristalsis; AP) (8, 17). AP is observed throughout gestation in avian and mammalian species both in culture and in tissue bath, and its frequency appears coupled to cultured lung growth (in vitro modulation of one leads to parallel changes in the other) (17, 21, 30, 31). ASM peristalsis appears therefore to be yet another mechanical stimulus to lung development (22). Further support for a role of ASM in lung growth derives from the observation that, within the embryonic lung mesenchyme, it is ASM progenitors that produce the fibroblast growth factor-10 (FGF-10) required for normal epithelial growth and branching (23). Finally, when lung growth is impaired, ASM abnormalities coincide: human congenital diaphragmatic hernia (CDH; ~1:2,500 births) remains a premier example where hypoplastic lung growth is responsible for significant death (~50%) and disability (34). This human lung hypoplasia accompanies abnormal expression of serum response factor (SRF) isoforms with impairment of SRF-mediated, ASM-specific gene expression (38). Nitrofen administration to pregnant rats leads to pulmonary hypoplasia in all pups and CDH in a proportion (18). ASM in this CDH model exhibits abnormal force generation and impaired relaxation near term (3).

Four properties of the nitrofen CDH model permit further scrutiny of the relationship between prenatal lung growth and ASM function. First, the lung hypoplasia is apparent from embryonic stages onward and before development of CDH (9, 16, 19). Therefore, we can test whether ASM dysfunction described near term in nitrofen-exposed lung is in fact apparent much earlier (and may therefore contribute to hypoplastic lung development) (3). Second, nitrofen administration at *day 9.5* of gestation impairs the left lung more than the right lung (20). We can further test links between peristalsis and growth by examining whether the spatial distribution of AP waves reflects this skewed growth. Third, FGF-10 is downregulated in, and induces remedial growth of, nitrofen-induced hypoplastic lung in vitro (1). If AP and growth are closely related, we postulate that FGF-10 rescue of lung hypoplasia will "normalize" ASM activity. Fourth, the nitrofen model permits the first examination of links between growth and AP where lung hypoplasia has been generated in vivo (17, 18).

Address for reprint requests and other correspondence: E. C. Jesudason, National Clinician Scientist in Pediatric Surgery, Institute of Child Health, Alder Hey Children's Hospital, Eaton Road, Liverpool, United Kingdom (e-mail: e.jesudason@liv.ac.uk).

The costs of publication of this article were defrayed in part by the payment of page charges. The article must therefore be hereby marked "*advertisement*" in accordance with 18 U.S.C. Section 1734 solely to indicate this fact.

MATERIALS AND METHODS

Generation and modulation of lung hypoplasia and peristalsis in culture. Timed-pregnant Sprague-Dawley rats (Charles River) were gavage fed 100 mg of nitrofen (Zheijang Chemicals) dissolved in olive oil on *day 9.5* of gestation (vaginal plug = *day 0*, term = *day 22.5*) to induce left-sided CDH and pulmonary hypoplasia in newborn pups (6, 16). Control animals received olive oil alone. Lung primordia were harvested on *day 13.5* of gestation and cultured on translucent membranes (Millicell; Millipore, Bedford, MA) for 78 h at 37°C in 5% (vol/vol) CO_2, as previously described (16). Lungs were cultured at the air-medium interface, bathed in serum-free culture medium [DMEM/F-12 (GIBCO-UK) with 100 IU/ml penicillin and 100 μg/ml streptomycin (GIBCO-BRL, UK) ± one of the following (or combination of 2 as explained in RESULTS)]: 5% (vol/vol) fetal calf serum, 50 ng/ml FGF-10, 0.1 μM nicotine (cholinergic agonist), 5 μM nifedipine (L-type calcium channel blocker) in DMSO, or 20 μM U0126 (non-competitive MEK1/2 inhibitor). Doses were derived from the literature (17), and culture medium was renewed at 48 h.

For each cultured lung, frequency of airway contractions was recorded over 10-min periods at 30, 54, and 78 h, with the contraction waves classified by their site of origin as L- (left lung), T- (tracheal), or R- (right lung) waves as described (17). All experimental procedures were approved and licensed by the UK Home Office.

Lung morphometry. Lung morphometry was performed as previously described (16). Briefly, lungs were photographed after 30, 54, and 78 h in culture using a Hamamatsu C7190-10 series dual mode cooled EB-charge-coupled device camera (Hamamatsu City, Japan) with a 5 × 0.25 numerical aperture Zeiss Fluar objective (Germany). Images were captured and processed using Kinetic Imaging AQM (Nottingham, UK) software that was also used to trace specimen outlines and calculate lung area and perimeter measurements after calibration with a graticule. Terminal lung bud counts were taken at 30, 54, and 78 h in culture.

Immunohistochemistry. Cultured lungs were fixed after 30, 54, and 78 h in 4% (wt/vol) paraformaldehyde (0.1 M PBS, pH 7.4), rinsed in PBS, cryoprotected with 20% (wt/vol) sucrose, and gelatin embedded [7.5% (wt/vol) gelatin, 15% (wt/vol) sucrose in PBS] before being covered in Cryo-M-Bed (Bright, UK) and snap frozen at −40°C. Lung sections were taken at 7 μm and mounted on chrome alum gel slides for storage at −40°C.

Slides were washed in 0.5% hydrogen peroxidase in 60% methanol to quench endogenous peroxidase and rinsed in distilled water. They were then incubated with α-SMA antibody (monoclonal anti-α-SMA clone no. 1A4, mouse, Sigma) at 1:500 dilution with 0.1% BSA in PBS overnight at 4°C. Slides were rinsed in PBS. Primary antibody was labeled with Strept ABComplex Duet Kit (Dako K0492) as per protocol and visualized with diaminobenzidine (D-0426 Sigma) as per kit protocol. Slides were then lightly counterstained with hematoxylin before being dehydrated, cleared, and mounted. Negative controls were performed in the absence of the primary antibody.

Statistical analysis. Proportions of lungs contracting and proportions of L-, T-, and R-waves were analyzed using the chi-squared test. Morphometry data (area, perimeter, and terminal bud counts) were non-normally distributed and were analyzed by Mann-Whitney's *U*-test for nonparametric data. Intercontraction intervals approximated to the normal distribution, and Student's *t*-test was used to compare means. Significance was taken as $P < 0.01$ unless otherwise documented. We used SPSS statistics package version 11.0 for Windows (SPSS, Chicago, IL).

RESULTS

Failed maturation of AP accompanies lung hypoplasia before CDH. AP is developmentally regulated. In normal control lungs at 30 h ($n = 26$), AP waves propagated primarily from the R-waves (Fig. 1, *top*). These vastly outnumbered those AP waves emerging from the left lung, which in turn exceeded those from the trachea. By 54 ($n = 31$) and 72 h ($n = 23$), T-waves peter out in normal control lung (Fig. 1, *middle* and *bottom*). Previous SMA immunostaining shows that the normal extinction of T-wave activity is not due to loss of proximal ASM (17). Moreover, when subsequently challenged with nicotine, proximal ASM from normal lung retains the competence to generate T-waves: nicotine significantly elevated T-wave activity in normal lung at 54 and 78 h ($n = 15$ at 54 h; $n = 13$ at 78 h; chi-squared test; Fig. 1, *top* to *bottom*).

Lung hypoplasia is associated with near-term and postnatal ASM-related dysfunction (3, 38). However, in the present study, hypoplastic lungs showed abnormal ASM activity far earlier during embryonic development. In nitrofen-exposed lung at 30 h ($n = 20$), L- rather than T-waves were least frequent (mirroring the greatest impairment of left lung growth in the model; Fig. 1); second, T-waves persisted in hypoplastic lung at 54 ($n = 52$) and 78 h ($n = 27$) despite having ceased in normal lung at the same times (Fig. 1). This failure of proximal ASM to quiesce in hypoplastic lung cannot be attributed simply to ASM maldistribution: SMA immunohistochemistry exhibited no differences between hypoplastic and normal lung (Fig. 2) (17). Moreover, persistence of T-waves in hypoplastic lung is inadequately explained by a global delay in ASM development. ASM peristalsis emerged similarly in hypoplastic and normal lungs: after 30-h culture, 16 of 47 hypoplastic lungs (34%) were peristalsing, whereas all hypoplastic lungs were undergoing peristalsis by 54 and 78 h [precisely matching onset in normal lungs (17)]. Arguing further against a simple developmental delay, the capacity of hypoplastic lung for abnormal late T-waves does not appear to decay: in contrast to normal lung, direct nicotine challenge of hypoplastic lung significantly elevated T-wave activity (to higher frequencies than L-waves) at 54 and 78 h ($n = 20$ at 54 h and $n = 12$ at 78 h; chi-squared test; Fig. 1).

We then showed that T-waves appear to persist in hypoplastic lung due to deficiency of FGF-10. Proximo-distal differentiation of the lung requires FGF-10 (13). Nitrofen-exposed lung features abnormal differentiation and FGF-10 downregulation (1, 7). FGF-10 treatment improves nitrofen-exposed lung growth in vitro (1). In the present study, FGF-10 treatment was associated with a normal pattern of L-, T-, and R-waves in control lung ($n = 14$ at 30 h; $n = 16$ at 54 and 78 h) (Fig. 1, *left*); however, in hypoplastic lung, FGF-10 significantly suppressed T-wave activity (chi-squared test), thereby completely normalizing the pattern of AP waves at 54 h ($n = 19$ at all time points; Fig. 1, *right*). Restoration of growth, therefore, accompanies restoration of normal patterns of AP activity. By 78 h, T-waves return albeit at a low level (perhaps related to change of FGF-10-containing medium at 48 h).

Hence, early hypoplastic lung features abnormal ASM activity before teratogenic CDH: the consistent but nonsignificant trend toward reduced L-wave activity (coincident with reduced left lung growth in the model) gives way to abnormal persistence of T-waves. Suppressed by FGF-10, abnormal T-waves persist without other overt abnormality of ASM distribution, maturation (timing of onset of AP), or responsiveness (cholinergic induction of T-waves).

Normal coupling of AP to lung growth is disrupted in hypoplastic lung. AP, therefore, develops abnormally in hypoplastic lung. We then showed that normal coupling between

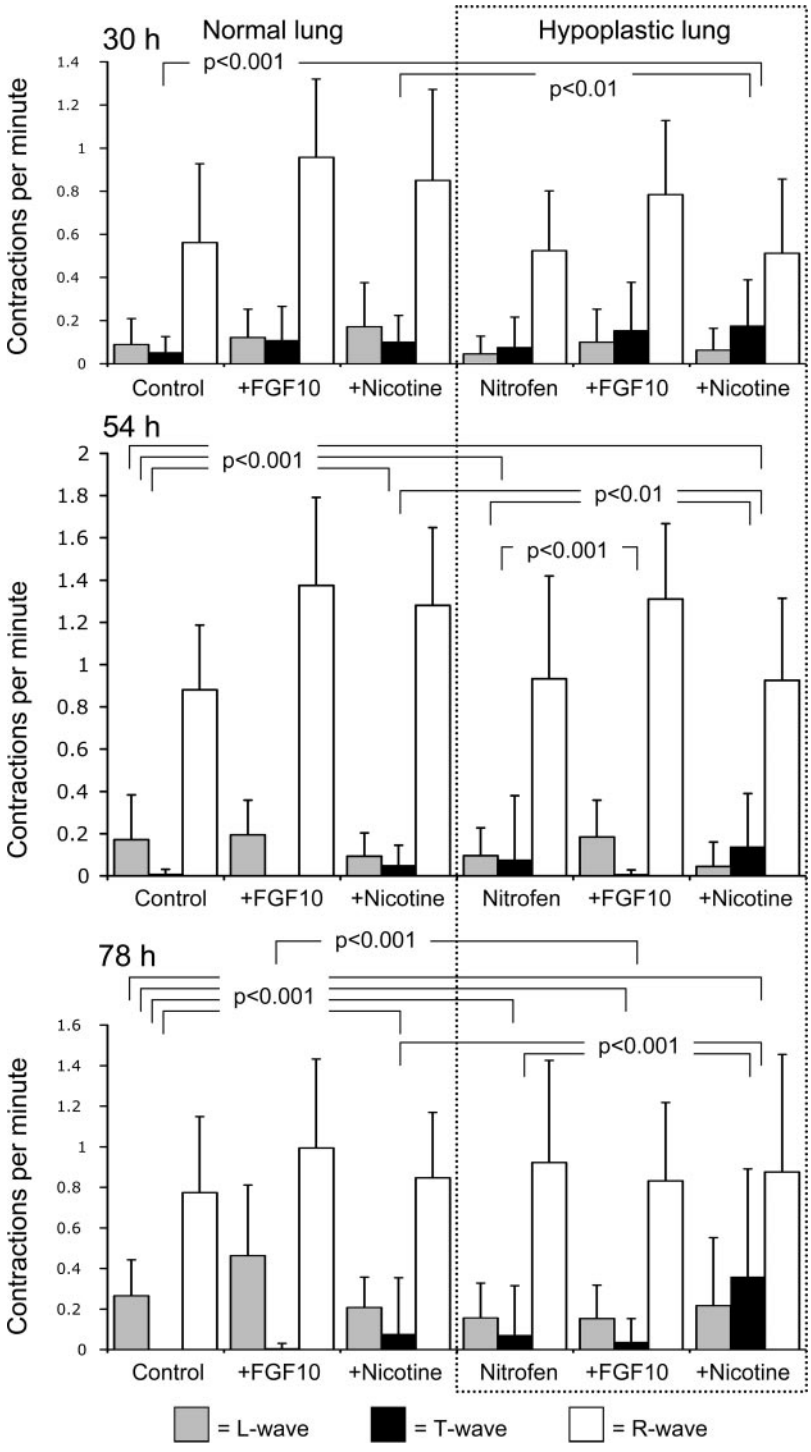

Fig. 1. Changing distribution of L- (left lung), T- (tracheal), and R- (right lung) waves with development, with lung hypoplasia, and with pharmacological manipulation. Shown are rates of contraction per minute commencing in the left lung (gray), trachea (black), and right lung (white) at 30 h (*top*), 54 h (*middle*), and 78 h (*bottom*) in vitro. Results are shown for nitrofen-exposed lungs (*right*, inside dotted box). Bars represent means and SD. T-waves disappear from normal lung during development. This process is impaired in hypoplastic lung. Nicotine administration also slows the decline in T-wave activity, whereas FGF-10 (fibroblast growth factor-10) appears to hasten it. Chi-squared testing determined significant differences in L-, T-, and R-wave distributions.

growth and AP is undone in nitrofen-induced lung hypoplasia by using the approach of alternately stimulating/inhibiting either AP or growth and measuring the effects on the other (as previously described) (17).

In normal lung, serum challenge, FGF-10 treatment, or nicotine increased both growth and AP activity (17). In contrast, only serum elicited this coupled response in hypoplastic lung. Compared with untreated hypoplastic lungs ($n = 47$), serum-treated hypoplastic lungs ($n = 18$) had increased lung area at 54 h, increased area, perimeter, and bud count at 78 h, and reduced intercontraction interval at 54 and 78 h (Figs. 3 and 4); in contrast, FGF-10 significantly increased area of hypoplastic lungs ($n = 12$) at 54 and 78 h, but reduced intercontraction intervals at only 54 h (Figs. 3 and 4); similarly, nicotine-treated hypoplastic lungs ($n = 12$) had a small increase in lung area at 54 h and a decrease in intercontraction interval at 78 h only (Figs. 3 and 4).

Nifedipine or U0126 (a MEK1/2 inhibitor) reduces growth and peristalsis in normal lung (17). In hypoplastic lung, nifedipine did not elicit a coupled response, whereas the effects of

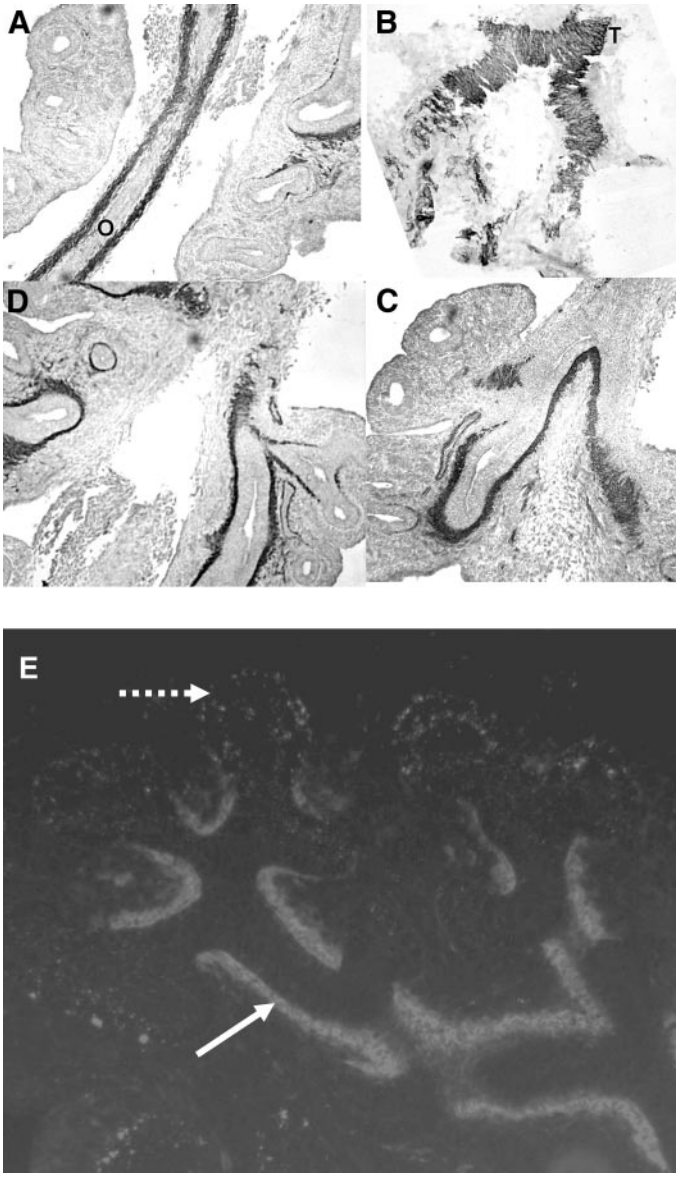

Fig. 2. Smooth muscle distribution in embryonic lung hypoplasia. Smooth muscle distribution is well documented in normal lung. However, *A* to *D* (clockwise) shows sections through a *day 14.5* nitrofen-exposed hypoplastic lung primordium progressing from dorsal to ventral. *A*: the esophagus (O) as an internal positive control (smooth muscle is stained black throughout *A–D* by α-smooth muscle immunochemistry). *B*: smooth muscle cells on the posterior trachea that are arrayed transversely to the airway's long axis. *C* and *D*: smooth muscle distributed along the proximal airways. Note the smooth muscle expression does not extend to the lung periphery at this stage; furthermore, smooth muscle predominates posteriorly in the trachea. *E*: gray scale fluorescence immunohistochemistry for α-smooth muscle actin: smooth muscle (light color) is distributed along the principal airways (solid arrow) but spares end buds (dashed arrow).

U0126 were more loosely tied than in normal lung. Compared with untreated hypoplastic lungs ($n = 47$), nifedipine-treated hypoplastic lungs ($n = 13$) exhibited no morphological differences after 30 h despite complete abolition of AP throughout the culture period (Fig. 3). Moreover, FGF-10 had no rescue effects on hypoplastic lung in the presence of nifedipine and the absence of AP. In normal lungs, U0126 reduces bud count, area, perimeter, prevalence, and frequency of AP at all time points (17). Compared with untreated hypoplastic lungs ($n = 47$), U0126-treated hypoplastic lungs ($n = 17$) featured only reduced area, frequency (Figs. 3 and 4), and prevalence of AP: 8/17 contracting (47%) vs. 47/47 (100%) at 54 and 78 h, respectively ($P < 0.001$; chi-squared test). Attempts to reverse U0126-mediated decline in contractile activity with 0.1 mM nicotine ($n = 15$) further reduced growth at 78 h (Fig. 3) and the prevalence of contracting lungs [nil contracting at 30 ($P < 0.01$) and 54 h ($P < 0.001$) and only 5/15 at 72 h ($P < 0.001$); chi-squared test].

Together, these data indicate that, compared with normal embryonic lung, hypoplastic nitrofen-exposed lungs have a weaker relationship between AP frequency and lung growth. Commensurate with this "uncoupling," hypoplastic lung growth itself does not reduce AP frequency. Thus nitrofen-induced lung hypoplasia impairs not only FGF-10-driven spatiotemporal maturation of ASM activity but also the normal coupling between ASM contractility and lung growth.

DISCUSSION

Far from being the appendix of the lung, ASM and its peristalsis are plausibly related to prenatal lung development, e.g., FGF-10 is simultaneously responsible for both airway branching and development of the ASM lineage (4, 23). AP within developing lung produces rhythmic fluid flux and stretch that, like other mechanical factors (fetal breathing movements, lung-liquid-induced stretch), may regulate prenatal lung growth (10, 14, 25–27, 29, 35). Previous studies have demonstrated coupling of AP frequency and lung growth in vitro: pharmacological alteration of one consistently yields parallel changes in the other (and vice versa) (17). Finally, lung hypoplasia has been associated with perinatal ASM-related abnormalities (3, 38).

AP and the hypoplastic lung. Despite descriptions of AP dating back more than 80 years in a wide variety of species, the present study is the only one to report on peristaltic activity in abnormal lung (and to utilize this to decipher the links between AP and morphogenesis). We examined the spatiotemporal characteristics of AP and its relationship to lung growth in the nitrofen CDH model. This system has the particular benefits of asymmetric lung hypoplasia generated in vivo (left worse than right) (20), reduced FGF-10 expression (with rescue growth in response to FGF-10) (1), documented ASM dysfunction near term (3), and a pressing human correlate (CDH ~50% mortality) (34). We first showed that ASM behaves abnormally from the earliest stages of hypoplastic lung development (and before emerging CDH): T-waves are least frequent in normal lung, whereas initially L-waves are the least common in hypoplastic lung [commensurate with reported greater left lung hypoplasia (20)]; T-waves normally disappear with time, but in hypoplastic lung they persist. Second, normal coupling between growth and peristaltic contractility is undone in nitrofen-induced lung hypoplasia. Stimulation (serum, FGF-10, nicotine) and inhibition (nifedipine, U0126) studies no longer secure consistent parallel modulation of growth and AP. The reduced susceptibility of nitrofen-exposed lung growth to U0126-mediated inhibition may even indicate a preexisting lesion of MEK1/2 signaling in lung hypoplasia.

In the course of these experiments, we have demonstrated that normal ASM peristalsis is developmentally regulated:

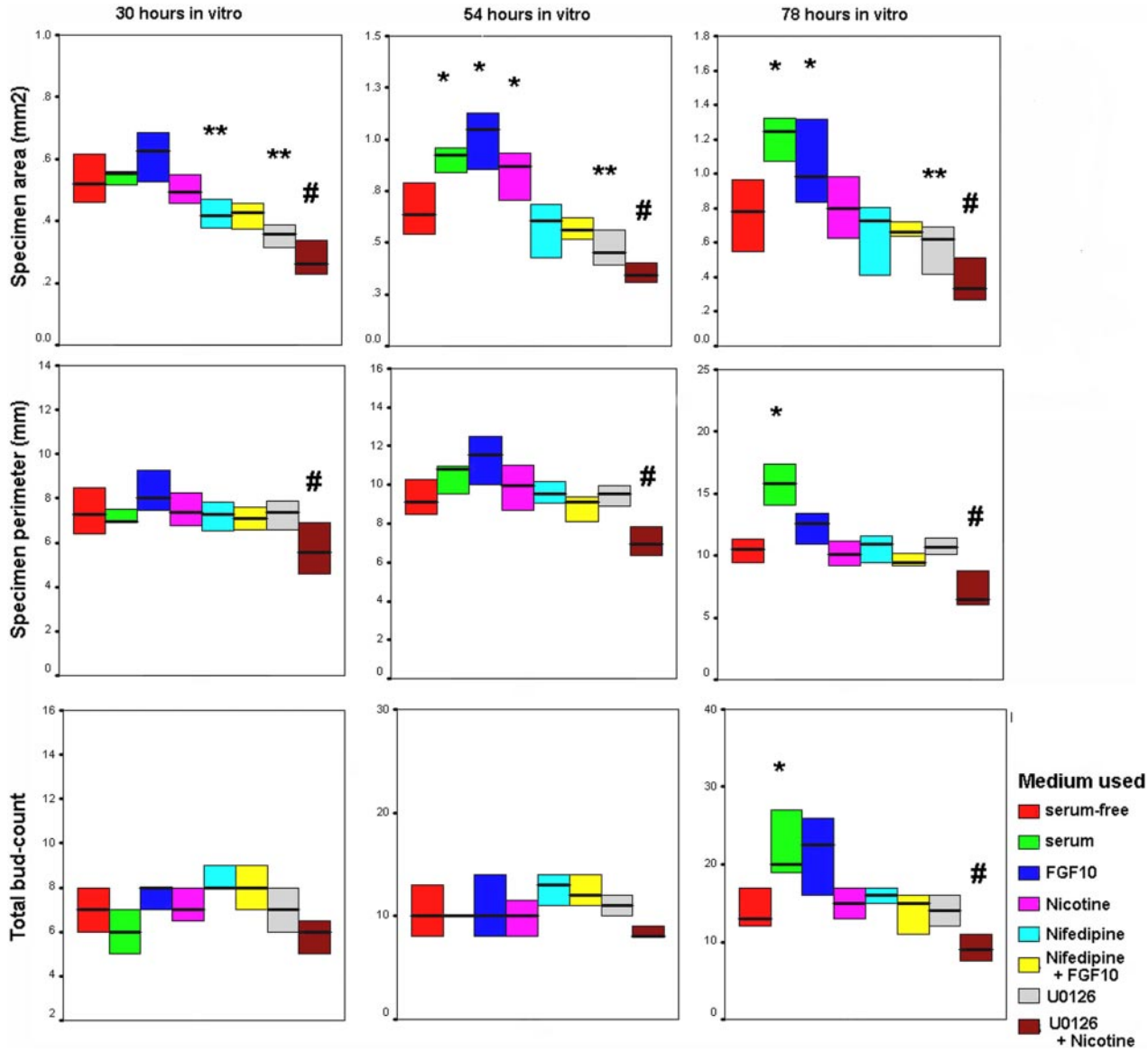

Fig. 3. Pharmacological manipulation of growth in hypoplastic lung. Morphometric data for nitrofen-exposed hypoplastic lungs cultured in serum-free medium (red), with serum (green); FGF-10 (blue); nicotine (purple); nifedipine (cyan); nifedipine + FGF-10 (yellow); U0126 (gray); and U0126 + nicotine (maroon). Box plot graphs show area (*top*), perimeter (*middle*), and total bud count (*bottom*) of lungs at 30 h (*left*), 54 h (*middle*), and 78 h (*right*) in vitro. Bars represent median and boxes' interquartile range. *Significant increase compared with serum-free medium; **significant decrease; #significant decrease compared with U0126 alone ($P < 0.01$, Mann-Whitney's *U*-test).

early T-wave activity is gradually replaced by L- and R-waves. This process is retarded in FGF-10-deficient hypoplastic lungs but can be restored (along with growth) by exogenous FGF-10. Together, this indicates that in addition to supporting proximodistal differentiation of lung epithelium (13), FGF-10 induces maturational changes in ASM behavior (and in particular the "centrifugal" migration of AP wave origins). Given the epithelial localization of its cognate receptor FGFR2IIIb, FGF-10's effects on ASM are likely to be indirect (17, 23). Nevertheless, these findings further support the link between FGF-10 and ASM biology (23). To check whether abnormal maturation of ASM activity in hypoplastic lung merely results from a gross lesion of ASM elaboration, we first used immunohistochemistry to establish normal and comparable patterns of SMA expression (17). Second, we showed that the emergence of AP was similar in normal and hypoplastic lungs (17). Third, we established that at later time points, proximal ASM in normal and hypoplastic lung retained similar capability to generate AP waves under cholinergic stimulation. These data indicate certain basic features of ASM ontology are preserved in lung hypoplasia. It remains to be seen whether, despite these several similarities, other features of ASM development (e.g., ASM bundle thickness, myosin isoforms) can explain abnormal ASM peristalsis (±growth) in lung hypoplasia.

Mechanisms for developmental maturation of AP activity. The present studies also yield insight into mechanisms governing normal maturation of early ASM activity. Nicotine reduced the ratio of L- to T-waves in normal lung: this distribution of L-, T-, and R-waves, therefore, mimics that observed in early normal lung culture and in nitrofen-induced

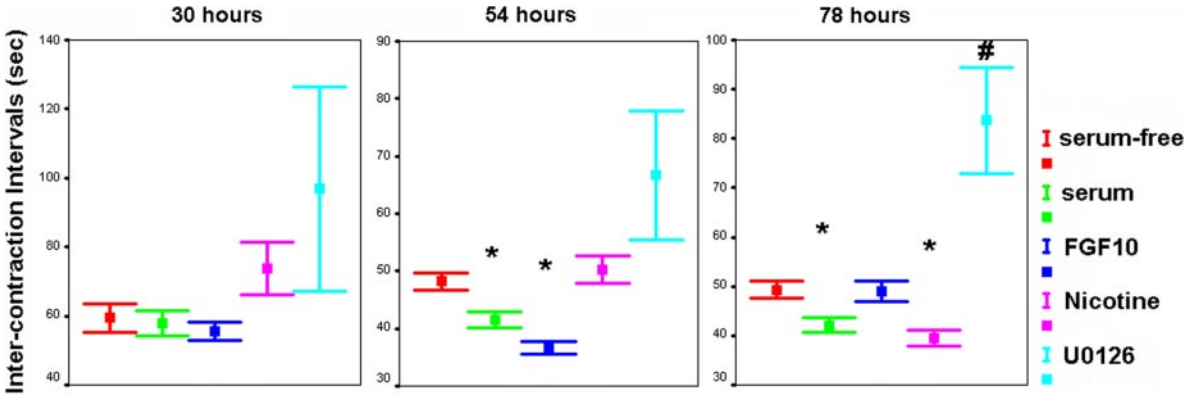

Fig. 4. Pharmacological manipulation of peristalsis in hypoplastic lung graphs depicting intercontraction intervals (seconds) at 30 h (*left*), 54 h (*middle*), and 78 h (*right*) in vitro. Data are shown for nitrofen-exposed hypoplastic lungs cultured in serum-free medium (red); with fetal calf serum (green); FGF-10 (blue); nicotine (purple); and U0126 (cyan). Bars represent means ± SE. No lungs were contracting in the presence of U0126 and nicotine until 78 h (not shown). *Significant reduction in intercontraction interval compared with serum-free medium ($P < 0.01$); #significant increase in intercontraction interval compared with serum-free medium ($P < 0.01$) by Student's *t*-test.

lung hypoplasia. In contrast, FGF-10 leaves the distribution of L-, T-, and R-waves unaffected in normal lung and tends to normalize it in hypoplastic lung primordia. Hence the spatial origin of AP waves can be modulated not only by in vivo nitrofen exposure but also by soluble ligands in vitro. Moreover, these data demonstrate that pharmacological agents can combine similar effects on overall AP frequency with dissimilar loco-regional activity: nicotine and FGF-10 both increase normal AP frequency, yet the former stimulates tracheal activity, whereas the latter suppresses it (17). Together, these contrasting effects show that the mechanisms of action of nicotine and FGF-10 on ASM are quite distinct (17). Nicotine is a cholinergic agonist that can act on ASM both directly and indirectly (36). The effect of nicotine is to skew the distribution of L-, T-, and R-waves "proximally" toward that observed early in culture and locations where ASM is initially elaborated (17). Although consistent with direct action on ASM, it is entirely plausible that nicotine's ASM effects arise indirectly via activity on epithelial or neuronal intermediates. FGF-10 acts on FGFR2IIIb-bearing epithelia and therefore clearly modulates ASM indirectly (17, 23). During normal development, FGF-10 expression becomes restricted to the growing lung periphery (4). If FGF-10's effect on ASM is both indirect and local, FGF-10 would be expected to favor AP waves originating from more peripheral sites rather than the proximal tracheal region. Again, as predicted, this is indeed what we observed: in normal and even hypoplastic lungs cultured with FGF-10, centrally located T-waves give way to more "peripheral" R- and L-waves. Thus the normal developmental migration of AP wave origins away from the central trachea appears to be indirectly regulated by FGF-10 (inasmuch as it is retarded in the FGF-10-deficient nitrofen lung and is correctable by exogenous FGF-10). The effects of nicotine indicate that although normal maturation of AP wave origins is FGF-10 dependent, proximal ASM retains a capacity for commencing peristalsis when stimulated directly. Hence emerging quiescence of proximal ASM may be due to loss of an FGF-10-dependent epithelial signal rather than an intrinsic loss of ASM competence (12). In this explanatory framework, the failure of proximal ASM activity to subside in hypoplastic lung (despite FGF-10 deficiency) may indicate a fundamental lesion of hypoplastic lung ASM (e.g., abnormal calcium signaling) and/or represent a relative failure of ASM in the FGF-10-deficient periphery to compete.

Developmental regulation of ASM contractility therefore appears to be subject to the same epithelial-mesenchymal interactions that direct morphogenesis. This concept lends credence to the role of epithelial-mesenchymal trophic units in postnatal ASM hyperreactivity (11). Future studies will seek to test this further by identifying, e.g., whether transplantation of peripheral mesenchyme on to proximal tracheal epithelium resurrects "T-waves" even at later stages in culture (2).

Clinical implications of abnormal ASM in lung hypoplasia. The role of dysfunctional ASM in the pathogenesis of lung hypoplasia deserves consideration at this point. Increased incidence of reactive airways disease in CDH survivors indicates a link with ASM problems (33, 37). Presumed to represent sequelae of barotrauma, such bronchial hyperresponsiveness may alternatively have its origins in abnormal ASM behavior prenatally. Given recent data unifying FGF-10-mediated lung growth and differentiation of ASM progenitors, it is reasonable to suggest that lesions of ASM development and function may accompany fundamental problems of early lung growth (23). We postulate that ASM elaboration helps regulate prenatal lung compliance to maintain pressures during FGF-10-driven expansion of luminal volume (15). Hence, in lung hypoplasia, an early mesenchymal lesion impairs ASM progenitors and hence FGF-10-mediated lung growth. Persisting ASM dysfunction then further hampers lung growth due to dysregulated compliance (and also explains the greater susceptibility to barotrauma witnessed in human hypoplastic lung) (28).

In conclusion, prenatal airway peristalsis is developmentally regulated during lung growth in a manner that appears to depend on FGF-10 and epithelial-mesenchymal interactions and is opposed by cholinergic agonist. Together with uncoupling of AP and growth, this maturation is disrupted in lung hypoplasia. These ASM changes predate CDH in this model. Abnormal ASM may therefore underlie aspects of early hypoplastic lung morphogenesis: we propose that ASM normally regulates prenatal lung compliance to maintain intraluminal pressures within the expanding lung. Testing this hypothesis

may yet allow us to answer the question: Does ASM have a purpose?

GRANTS

This work was funded by The Academy of Medical Sciences/Health Foundation, The Royal College of Surgeons of England, and The Birth Defects Foundation.

REFERENCES

1. **Acosta JM, Thebaud B, Castillo C, Mailleux A, Tefft D, Wuenschell C, Anderson KD, Bourbon J, Thiery JP, Bellusci S, and Warburton D.** Novel mechanisms in murine nitrofen-induced pulmonary hypoplasia: FGF-10 rescue in culture. *Am J Physiol Lung Cell Mol Physiol* 281: L250–L257, 2001.
2. **Alescio T.** The effect of the mesenchyme on epithelial morphogenesis in the in vitro development of mouse embryonal lung. *Arch Ital Anat Embriol* 73: 295–319, 1968.
3. **Belik J, Davidge ST, Zhang W, Pan J, and Greer JJ.** Airway smooth muscle changes in the nitrofen-induced congenital diaphragmatic hernia rat model. *Pediatr Res* 53: 737–743, 2003.
4. **Bellusci S, Grindley J, Emoto H, Itoh N, and Hogan BL.** Fibroblast growth factor 10 (FGF10) and branching morphogenesis in the embryonic mouse lung. *Development* 124: 4867–4878, 1997.
5. **Brusasco V and Pellegrino R.** Complexity of factors modulating airway narrowing in vivo: relevance to assessment of airway hyperresponsiveness. *J Appl Physiol* 95: 1305–1313, 2003.
6. **Cilley RE, Zgleszewski SE, Krummel TM, and Chinoy MR.** Nitrofen dose-dependent gestational day-specific murine lung hypoplasia and left-sided diaphragmatic hernia. *Am J Physiol Lung Cell Mol Physiol* 272: L362–L371, 1997.
7. **Coleman C, Zhao J, Gupta M, Buckley S, Tefft JD, Wuenschell CW, Minoo P, Anderson KD, and Warburton D.** Inhibition of vascular and epithelial differentiation in murine nitrofen-induced diaphragmatic hernia. *Am J Physiol Lung Cell Mol Physiol* 274: L636–L646, 1998.
8. **Featherstone NC, Jesudason EC, Connell MG, Fernig DG, Wray S, Losty PD, and Burdyga TV.** Spontaneous propagating calcium waves underpin airway peristalsis in embryonic rat lung. *Am J Respir Cell Mol Biol* 33: 153–160, 2005.
9. **Guilbert TW, Gebb SA, and Shannon JM.** Lung hypoplasia in the nitrofen model of congenital diaphragmatic hernia occurs early in development. *Am J Physiol Lung Cell Mol Physiol* 279: L1159–L1171, 2000.
10. **Harding R and Hooper SB.** Regulation of lung expansion and lung growth before birth. *J Appl Physiol* 81: 209–224, 1996.
11. **Holgate ST, Lackie PM, Howarth PH, Roche WR, Puddicombe SM, Richter A, Wilson SJ, Holloway JW, and Davies DE.** Invited lecture: activation of the epithelial mesenchymal trophic unit in the pathogenesis of asthma. *Int Arch Allergy Immunol* 124: 253–258, 2001.
12. **Hyatt BA, Shangguan X, and Shannon JM.** BMP4 modulates fibroblast growth factor-mediated induction of proximal and distal lung differentiation in mouse embryonic tracheal epithelium in mesenchyme-free culture. *Dev Dyn* 225: 153–165, 2002.
13. **Hyatt BA, Shangguan X, and Shannon JM.** FGF-10 induces SP-C and Bmp4 and regulates proximal-distal patterning in embryonic tracheal epithelium. *Am J Physiol Lung Cell Mol Physiol* 287: L1116–L1126, 2004.
14. **Ingber DE.** Mechanical control of tissue growth: function follows form. *Proc Natl Acad Sci USA* 102: 11571–11572, 2005.
15. **Jesudason EC.** Small lungs and suspect smooth muscle: congenital diaphragmatic hernia and the smooth muscle hypothesis. *J Pediatr Surg* 41: 431–435, 2006.
16. **Jesudason EC, Connell MG, Fernig DG, Lloyd DA, and Losty PD.** Early lung malformations in congenital diaphragmatic hernia. *J Pediatr Surg* 35: 124–127, 2000.
17. **Jesudason EC, Smith NP, Connell MG, Spiller DG, White MR, Fernig DG, and Losty PD.** Developing rat lung has a sided pacemaker region for morphogenesis-related airway peristalsis. *Am J Respir Cell Mol Biol* 32: 118–127, 2005.
18. **Kluth D, Kangah R, Reich P, Tenbrinck R, Tibboel D, and Lambrecht W.** Nitrofen-induced diaphragmatic hernias in rats: an animal model. *J Pediatr Surg* 25: 850–854, 1990.
19. **Kluth D, Tenbrinck R, von Ekesparre M, Kangah R, Reich P, Brandsma A, Tibboel D, and Lambrecht W.** The natural history of congenital diaphragmatic hernia and pulmonary hypoplasia in the embryo. *J Pediatr Surg* 28: 456–462; discussion 462–453, 1993.
20. **Leinwand MJ, Tefft JD, Zhao J, Coleman C, Anderson KD, and Warburton D.** Nitrofen inhibition of pulmonary growth and development occurs in the early embryonic mouse. *J Pediatr Surg* 37: 1263–1268, 2002.
21. **Lewis M.** Spontaneous rhythmical contraction of the muscles of the bronchial tubes and air sacs of the chick embryo. *Am J Physiol* 68: 385–388, 1924.
22. **Liu M, Tanswell AK, and Post M.** Mechanical force-induced signal transduction in lung cells. *Am J Physiol Lung Cell Mol Physiol* 277: L667–L683, 1999.
23. **Mailleux AA, Kelly R, Veltmaat JM, De Langhe SP, Zaffran S, Thiery JP, and Bellusci S.** Fgf10 expression identifies parabronchial smooth muscle cell progenitors and is required for their entry into the smooth muscle cell lineage. *Development* 132: 2157–2166, 2005.
24. **Mitzner W.** Airway smooth muscle: the appendix of the lung. *Am J Respir Crit Care Med* 169: 787–790, 2004.
25. **Moore KA, Polte T, Huang S, Shi B, Alsberg E, Sunday ME, and Ingber DE.** Control of basement membrane remodeling and epithelial branching morphogenesis in embryonic lung by Rho and cytoskeletal tension. *Dev Dyn* 232: 268–281, 2005.
26. **Nakamura KT and McCray PB Jr.** Fetal airway smooth-muscle contractility and lung development. A player in the band or just someone in the audience? *Am J Respir Cell Mol Biol* 23: 3–6, 2000.
27. **Nelson CM, Jean RP, Tan JL, Liu WF, Sniadecki NJ, Spector AA, and Chen CS.** Emergent patterns of growth controlled by multicellular form and mechanics. *Proc Natl Acad Sci USA* 102: 11594–11599, 2005.
28. **Sakurai Y, Azarow K, Cutz E, Messineo A, Pearl R, and Bohn D.** Pulmonary barotrauma in congenital diaphragmatic hernia: a clinicopathological correlation. *J Pediatr Surg* 34: 1813–1817, 1999.
29. **Schittny JC, Miserocchi G, and Sparrow MP.** Spontaneous peristaltic airway contractions propel lung liquid through the bronchial tree of intact and fetal lung explants. *Am J Respir Cell Mol Biol* 23: 11–18, 2000.
30. **Schopper W.** Embryonales underwachsenes Lungengewebe vom Meerschweinchen und Huhn in der Kultur mit Zeitrafferbeobachtungen an Flimmerepithel, sog. Alveolarphagocyten und von Kontraktionen der Bronchialmuskulatur. *Virchows Arch* 295: 623–644, 1935.
31. **Schopper W.** Uber das Verhalten des Lungengewebes in der Gewebekultur (Filmdemonstration). *Arch Exptl Zellforsch* 19: 326–328, 1937.
32. **Seow CY and Fredberg JJ.** Historical perspective on airway smooth muscle: the saga of a frustrated cell. *J Appl Physiol* 91: 938–952, 2001.
33. **Skousgaard SG.** Severe bronchial hyperreactivity as a sequel to congenital diaphragmatic hernia. *Paediatr Anaesth* 8: 503–505, 1998.
34. **Smith NP, Jesudason EC, Featherstone NC, Corbett HJ, and Losty PD.** Recent advances in congenital diaphragmatic hernia. *Arch Dis Child* 90: 426–428, 2005.
35. **Sparrow MP and Lamb JP.** Ontogeny of airway smooth muscle: structure, innervation, myogenesis and function in the fetal lung. *Respir Physiol Neurobiol* 137: 361–372, 2003.
36. **Takayanagi I, Kizawa Y, and Sone H.** Action of nicotine on guinea-pig isolated bronchial smooth muscle preparation. *Gen Pharmacol* 15: 349–352, 1984.
37. **Vanamo K, Rintala R, Sovijarvi A, Jaaskelainen J, Turpeinen M, Lindahl H, and Louhimo I.** Long-term pulmonary sequelae in survivors of congenital diaphragmatic defects. *J Pediatr Surg* 31: 1096–1099; discussion 1099–1100, 1996.
38. **Yang Y, Beqaj S, Kemp P, Ariel I, and Schuger L.** Stretch-induced alternative splicing of serum response factor promotes bronchial myogenesis and is defective in lung hypoplasia. *J Clin Invest* 106: 1321–1330, 2000.